

DRAG INSTABILITY IN THE MODIFIED BETATRON

P. SPRANGLE AND C. A. KAPETANAKOS

Naval Research Laboratory, Washington, D.C. 20375 U.S.A.

(Received February 10, 1983; in final form April 1983)

The instability discussed in this report is a special case of the resistive-wall instability. It occurs when the beam current that propagates inside a resistive vacuum chamber along an external toroidal magnetic field exceeds a critical value. The drag instability is characterized by uniform density in the direction of propagation, i.e., the toroidal wave number is zero. We have studied the drag instability over a wide range of parameters, including the limit $\delta > (b - a)$, where δ is the skin depth and $(b - a)$ is the thickness of the conducting wall. This limit is relevant to the proof-of-principle experiment on the modified betatron accelerator presently under design at the Naval Research Laboratory.

I. INTRODUCTION

Currently there are studies at several laboratories¹⁻¹³ to assess the feasibility of developing ultra-high current electron accelerators. Such devices have potential applications in several areas including high-energy physics, the fusion program and the generation of coherent, short-wavelength electromagnetic radiation.

Prominent among the various contemplated devices that are suitable for the generation of ultra-high current electron beams is the modified betatron.⁴⁻¹³ This device consists of a conventional betatron magnetic-field configuration as well as a strong toroidal magnetic field. In general, the toroidal field has a number of important beneficial effects on the stability of the circulating electron ring. However, there are a number of drawbacks associated with the addition of the toroidal magnetic field, one among them is the instability analyzed and discussed in the present paper.

When an electron ring is confined in a modified betatron field configuration within perfectly conducting walls, the centroid of the relativistic ring can experience, in addition to magnetic forces that are related to the external fields, forces that are associated with the induced charges and currents on the conducting wall as well as hoop forces. The hoop forces have their origin in the finite radius of curvature of the electron orbits and have been treated previously,^{8,17} In the present analysis, the hoop forces are neglected, i.e., the torus is unwrapped into a straight infinite long cylinder.

When the resistivity of the circular cross-section wall surrounding the electron ring is zero, the induced charge and current forces are directed transverse to the wall. However, when the resistivity is finite, the decay of the wall currents produces an additional magnetic-field component that is directed towards the wall. As shown in Fig. 1, the force, $F_d = -|e|V_\theta B_\phi$ associated with the additional component of magnetic field is always directed opposite to the velocity vector of the slow rotation of the centroid ($\mathbf{V}_B = \rho \boldsymbol{\omega}_B =$ bounce velocity) and thus can be called a drag force. If both the toroidal magnetic field ($B_{0\theta}$) and the bounce frequency ω_B are positive, the drift velocity $\mathbf{V}_D = -(\mathbf{F}_d \times \mathbf{B}_{0\theta})/|e|B_{0\theta}^2$ is negative and thus the drag force results in a stable, inward spiraling motion of the beam centroid. However, when $B_{0\theta} > 0$ but $\omega_B < 0$, the drift velocity is positive, resulting in an instability and the beam centroid spirals outward.

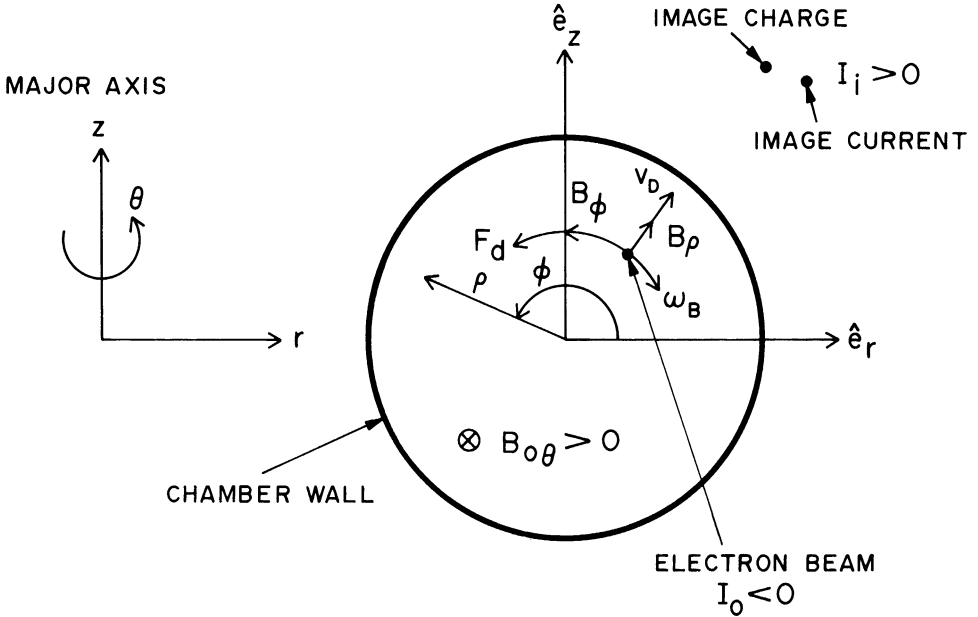


FIGURE 1 Minor cross section of modified betatron showing beam-center motion, image charge, image current, induced magnetic field and drag force on the beam. The drag instability is stable if $\omega_B B_{0\theta}/|B_{0\theta}| > 0$ and unstable if $\omega_B B_{0\theta}/|B_{0\theta}| < 0$.

The drag force has its origin in the decay of wall currents and more specifically in the polarity change of the wall currents at the end of the beam pulse. This may be seen by considering the simpler case of a straight beam propagating along and near the surface of a plane conductor. The wall currents are driven by inductive electric fields $E_\theta = -1/c(\partial A_\theta/\partial t)$, where A_θ is the magnetic vector potential. Integrating this equation and using Ohm's law, we get $\int_0^\infty J_\theta dt = 0$, provided $A_\theta(t=0) - A_\theta(t=\infty) = 0$. Thus, as the electron beam passes near a certain section of the conductor, the image current has the opposite polarity of the beam current. However, the polarity of the image currents on the section of the cylindrical conductor near which the rotating electron beam passed earlier is the same as that of the beam. As a result, a drag force is developed that is directed opposite to V_B .

The drag instability discussed here is a special case of the resistive-wall instability.^{17,18} This instability is characterized by uniform density in the direction of propagation and is present even when the toroidal magnetic field is zero.¹⁹ With a magnetic field along the direction of propagation, the instability has been treated²⁰ in the limit $\delta \ll b - a$, where δ is the skin depth and $b - a$ is the thickness of the conducting wall. In the present paper, we have studied the drag instability over a wide range of parameters. Special attention was focused on the limit $\delta > (b - a)$. This limit is relevant to the proof-of-principle modified betatron accelerator presently under design at the Naval Research Laboratory.

The drag instability in the modified betatron is distinct from the beam-orbit instability, which may arise even for an infinite chamber-wall conductivity. The origin of the beam-orbit instability^{8,10} is due to an imbalance in the various confining forces resulting in a net transverse drift velocity of the beam's center, and occurs even in the absence of dissipative forces. On the other hand, the drag instability arises from

dissipative effects, i.e., finite conductivity. For a linear beam propagating through a straight chamber of finite conductivity, the drag instability is always unstable. The forces responsible for the stabilization of this instability arise from curvature effects.

II. THE MODEL

A cross-sectional view of the electron beam within the conducting cylinder is shown in Fig. 2. The inner and outer radius of the thin cylinder is respectively a and b where $b - a \ll a$. The finite conductivity of the cylinder is denoted by σ . The number density n_0 and current density $\mathbf{J}_0 = -|e|n_0v_0\hat{e}_z$ of the beam are assumed to be spatially uniform. In addition the electron beam is assumed to be in rigid transverse motion within the cylinder. The position of the beam center with respect to the center of the cylinder is

$$\Delta(t) = \Delta r(t)\hat{e}_x + \Delta z(t)\hat{e}_y, \quad (1)$$

where $\Delta r(t) = \Delta(t) \cos \alpha(t)$ and $\Delta z(t) = \Delta(t) \sin \alpha(t)$. In what follows we assume that the beam cross section remains circular with radius $r_b \ll a$.

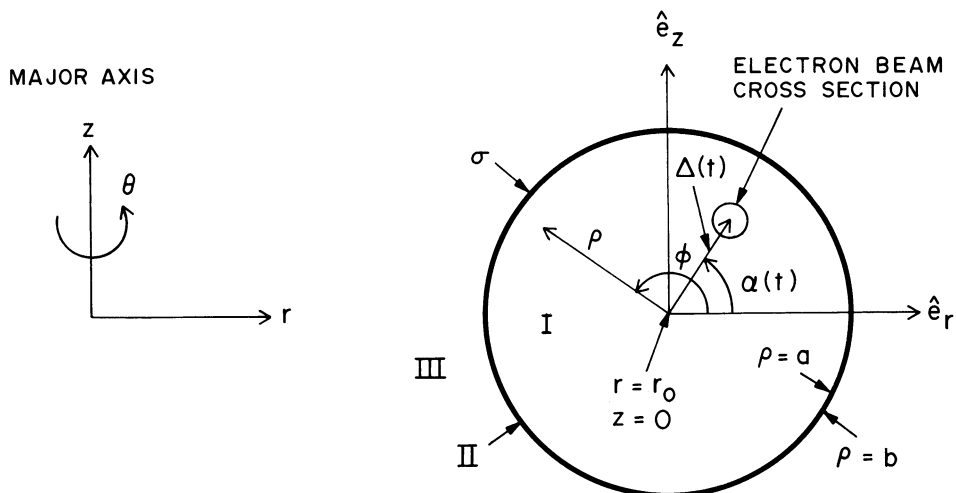


FIGURE 2 Minor cross section of modified betatron showing polar coordinates (ρ, ϕ) and center of beam orbit $(\Delta(t), \alpha(t))$. The cross section of the torus is partitioned into three regions, I, II and III.

III. INDUCED MAGNETIC FIELD

The induced magnetic field at the center of the beam is derivable from the vector potential in region I of Fig. 2. Only the axial component of the vector potential will be considered here, since it is assumed that the transverse beam velocity is much less than c , while the toroidal velocity (in the θ -direction) is close to c . The solution of the wave equation for the total vector potential in region I, A_T^I , consists of a particular solution as well as a homogeneous solution. The information concerning the boundary

conditions along the inner surface, $\rho = a$, resides in the homogeneous solution only. Furthermore, since the fields and therefore the forces associated with the particular solution vanish at the beam center, i.e., $\rho = \Delta(t)$, we are only interested in the homogeneous solution of the vector potential in region I. However, to obtain the homogeneous solution in region I, the full solution is needed, together with the appropriate boundary conditions on \mathbf{A}_T^I and $\partial A_T^I / \partial \rho$ at $\rho = a$. Since the particular solution of the vector potential is needed only along the inner surface of the cylinder, we may represent the electron beam by a line current. Neglecting the displacement current, the particular solution becomes

$$\mathbf{A}_p^I(\rho, \phi, t) = \frac{-2I(t)}{c} \ln|\rho - \Delta(t)| \hat{e}_\theta, \quad (2)$$

where

$$|\rho - \Delta(t)| = [\rho^2 + \Delta^2(t) - 2\rho\Delta(t) \cos(\phi - \alpha(t))]^{1/2}, \quad (3)$$

and $I(t) = -|e|n_0v_0\pi r_b^2$ is the beam current. The homogeneous solution in region I has the general form

$$\mathbf{A}_h^I(\rho, \phi, t) = \sum_{l=0}^{\infty} a_l^I(t)(\rho/a)^l e^{il\phi} \hat{e}_\theta + c.c., \quad (4)$$

where the time-dependent coefficients a_l^I are to be determined by applying the appropriate boundary conditions at $\rho = a$. The induced magnetic field components, derivable from \mathbf{A}_h^I , are

$$B_\rho(\rho, \phi, t) = -\sum_{l=1}^{\infty} \frac{il}{a} a_l^I(t)(\rho/a)^{l-1} e^{il\phi} + c.c., \quad (5a)$$

and

$$B_\phi(\rho, \phi, t) = +\sum_{l=1}^{\infty} \frac{l}{a} a_l^I(t)(\rho/a)^{l-1} e^{il\phi} + c.c.. \quad (5b)$$

The induced magnetic field at the beam's center is obtained by setting $\rho = \Delta(t)$ and $\phi = \alpha(t)$ in Eq. (5). Adding Eqs. (2) and (4), we find that the total vector potential in region I, for $a \geq \rho > \Delta(t)$, can be written as

$$\begin{aligned} A_T^I(\rho, \phi, t) = & \left(a_0^I(t) - \frac{I(t)}{c} \ln \rho \right) \hat{e}_\theta \\ & + \sum_{l=1}^{\infty} \left\{ a_l^I(t) \left(\frac{\rho}{a} \right)^l + \frac{I(t)}{c} l^{-1} \left(\frac{\Delta(t)}{\rho} \right)^l e^{-il\alpha} \right\} e^{il\phi} \hat{e}_\theta + c.c.. \end{aligned} \quad (6)$$

In obtaining Eq. (6), we made use of the expansion

$$\ln(\rho^2 + \Delta^2 - 2\rho\Delta \cos(\phi - \alpha))^{1/2} = \frac{1}{2} \ln \rho - \frac{1}{2} \sum_{l=1}^{\infty} l^{-1} \left(\frac{\Delta}{\rho} \right)^l e^{il(\phi - \alpha)} + c.c.,$$

which is valid for $\rho > \Delta$.

In region II the axial component of the vector potential satisfies the diffusion equation

$$\nabla^2 \mathbf{A}^{II} = \frac{4\pi\sigma}{c^2} \frac{\partial \mathbf{A}^{II}}{\partial t}, \quad (7)$$

where the displacement current has been neglected. Since we are considering a thin cylinder, $b - a \ll a$, we can replace ∇^2 with $\partial^2/\partial\rho^2 - a^{-2}\partial^2/\partial\phi^2$; i.e., a Cartesian representation is used within the cylinder. The vector potential \mathbf{A}^{II} may be represented by the form

$$\mathbf{A}^{II}(\rho, \phi, t) = \sum_{l=0}^{\infty} a_l^{II}(\rho, t) e^{il\phi} \hat{e}_\theta + c.c.. \quad (8)$$

Substituting Eq. (8) into Eq. (7) and denoting the temporal Laplace transform of $a_l^{II}(\rho, t)$ by $\tilde{a}_l^{II}(\rho, s)$, we find that

$$\begin{aligned} \tilde{a}_l^{II}(\rho, s) = \tilde{a}_l^{II}(a, s) \frac{\sinh[\mu_l(s)(b - \rho)/(b - a)]}{\sinh \mu_l(s)} \\ + \tilde{a}_l^{II}(b, s) \frac{\sinh[\mu_l(s)(\rho - a)/(b - a)]}{\sinh \mu_l(s)}, \end{aligned} \quad (9)$$

where $\mu_l(s) = (b - a)(4\pi\sigma s/c^2 + l^2/a^2)^{1/2}$ and s is the Laplace Transform variable. In obtaining Eq. (9), we used the Cartesian representation for ∇^2 and the initial condition $a_l^{II}(\rho, t = 0) = 0$. Using the same representation for the vector potential in region III as was used in region II, i.e., Eq. (8) and solving the vacuum wave equation, in polar coordinates, with the displacement-current term included we find that $\tilde{a}_l^{III}(\rho, s)$ is

$$\tilde{a}_l^{III}(\rho, s) = \tilde{a}_l^{III}(b, s) K_l(s\rho/c)/K_l(sb/c), \quad (10)$$

where K_l is the modified Bessel function. The continuity of $\tilde{a}_l(\rho, s)$ is satisfied by Eqs. (9) and (10). From Eqs. (9) and (10), continuity of $\partial\tilde{a}_l(\rho, s)/\partial\rho$ across $\rho = a$ implies

$$\tilde{a}_l^{II}(b, s) = \tilde{f}_l(s) \tilde{a}_l^{II}(a, s), \quad (11)$$

where

$$\tilde{f}_l(s) = \frac{-(b/(b - a))\mu_l(s) \sinh^{-1} \mu_l(s)}{\left(l - \frac{sb}{c} K_{l+1}(sb/c)/K_l(sb/c) - (b/(b - a))\mu_l \coth \mu_l(s)\right)}. \quad (12)$$

Substituting Eq. (11) into Eq. (9) gives

$$\tilde{a}_l^{II}(\rho, s) = \frac{\sinh\left(\frac{b - \rho}{b - a} \mu_l(s)\right) + \tilde{f}_l(s) \sinh\left(\frac{\rho - a}{b - a} \mu_l(s)\right)}{\sinh \mu_l(s)} \tilde{a}_l^{II}(a, s), \quad (13)$$

where $l = 0, 1, 2, \dots$

We now impose the necessary boundary condition that A and $\partial A/\partial \rho$ be continuous across the boundary at $\rho = a$. By applying the boundary condition across $\rho = a$ to the fields in regions I and II, the following relationships between the coefficients are obtained

$$a_0^I(t) - \frac{I(t)}{c} \ln a = a_0^{II}(a, t) \quad (14a)$$

$$a_l^I(t) + \frac{I(t)}{c} l^{-1} \left(\frac{\Delta(t)}{a} \right)^l e^{-il\alpha(t)} = a_l^{II}(a, t) \quad (14b)$$

$$-\frac{I(t)}{ac} = \left. \frac{\partial a_0^{II}(\rho, t)}{\partial \rho} \right|_{\rho=a}, \quad (14c)$$

and

$$\frac{l}{a} a_l^I(t) - \frac{I(t)}{ac} \left(\frac{\Delta(t)}{a} \right)^l e^{-il\alpha(t)} = \left. \frac{\partial a_l^{II}(\rho, t)}{\partial \rho} \right|_{\rho=a}, \quad (14d)$$

where $l = 1, 2$. Taking the Laplace transform of Eq. (14) and using Eq. (13), we find the relationships

$$\tilde{a}_0^I(s) - \frac{I_0}{sc} \ln a = \tilde{a}_0^{II}(a, s) \quad (15a)$$

$$\tilde{a}_l^I(s) + \frac{I_0}{c} l^{-1} \left(\frac{\Delta\tilde{r}(s)}{a} - i \frac{\Delta\tilde{z}(s)}{a} \right)^l = \tilde{a}_l^{II}(a, s) \quad (15b)$$

$$-\frac{I_0}{sc} = \tilde{F}_0(s) \tilde{a}_0(a, s), \quad (15c)$$

$$l\tilde{a}_l^I(s) - \frac{I_0}{c} \left(\frac{\Delta\tilde{r}(s)}{a} - i \frac{\Delta\tilde{z}(s)}{a} \right)^l = \tilde{F}_l(s) \tilde{a}_l^I(a, s) \quad (15d)$$

where $l = 1, 2$ and

$$\tilde{F}_l(s) = \frac{a\mu_l(s)}{(b-a) \sinh \mu_l(s)} (\tilde{f}_l(s) - \cosh \mu_l(s)). \quad (16)$$

In obtaining Eq. (15), we have taken the beam current to be of the form

$$I(t) = I_0 \theta(t),$$

where θ is the usual Heaviside unit step function and I_0 is the current amplitude. Solving Eq. (15) for the coefficients of the homogeneous part of the vector potential in region I gives

$$\tilde{a}_l^I(s) = \tilde{G}_l(s) \left(\frac{\Delta\tilde{r}(s)}{a} - i \frac{\Delta\tilde{z}(s)}{a} \right)^l, \quad (17)$$

where

$$\tilde{G}_l(s) = \begin{cases} s^{-1}(\ln a - \tilde{F}_l^{-1}(s)) & \text{for } l = 0 \\ l^{-1}(\tilde{F}_l(s) + l)/(\tilde{F}_l(s) - l) & \text{for } l = 1, 2. \end{cases} \quad (18a)$$

and

$$\tilde{F}_l(s) = -\frac{a}{b-a} \mu_l(s) \tanh \mu_l(s) \left(\frac{l \coth \mu_l + \frac{b}{b-a} \mu_l(s)}{l \tanh \mu_l + \frac{b}{b-a} \mu_l(s)} \right). \quad (18b)$$

Using Eq. (17), the induced magnetic field given by Eq. (5) becomes

$$B_\rho(\rho, \phi, t) = -\frac{I_0}{c} \sum_{l=1}^{\infty} \frac{il}{a} \left(\frac{\rho}{a}\right)^{l-1} e^{il\phi} \int_0^t G_l(t-\tau) \left(\frac{\Delta r(\tau)}{a} - \frac{i\Delta z(\tau)}{a}\right)^l d\tau + c.c., \quad (19a)$$

$$B_\phi(\rho, \phi, t) = +\frac{I_0}{c} \sum_{l=1}^{\infty} \frac{l}{a} \left(\frac{\rho}{a}\right)^{l-1} e^{il\phi} \int_0^t G_l(t-\tau) \left(\frac{\Delta r(\tau)}{a} - \frac{i\Delta z(\tau)}{a}\right)^l d\tau + c.c., \quad (19b)$$

where $G_l(t)$ is the inverse Laplace transform of $\tilde{G}_l(s)$ and $\Delta r(t)$, $\Delta z(t)$ are the coordinates of the beam's center. In order to study the beam dynamics, it is convenient to express the induced fields in a coordinate system defined by the unit vectors \hat{e}_r and \hat{e}_z . In this system, $B_r = B_\rho \cos \phi - B_\phi \sin \phi$ and $B_z = B_\rho \sin \phi + B_\phi \cos \phi$ and by using Eq. (19), we find that

$$B_r(r, z, t) = -i \frac{I_0}{c} \sum_{l=1}^{\infty} \frac{l}{a} \left(\frac{\rho}{a}\right)^{l-1} e^{i(l-1)\phi} \int_0^t G_l(t-\tau) \left(\frac{\Delta r(\tau)}{a} - \frac{i\Delta z(\tau)}{a}\right)^l d\tau + c.c., \quad (20a)$$

and

$$B_z(r, z, t) = \frac{I_0}{c} \sum_{l=1}^{\infty} \frac{l}{a} \left(\frac{\rho}{a}\right)^{l-1} e^{i(l-1)\phi} \int_0^t G_l(t-\tau) \left(\frac{\Delta r(\tau)}{a} - \frac{i\Delta z(\tau)}{a}\right)^l d\tau + c.c., \quad (20b)$$

where $\rho = ((r - r_0)^2 + z^2)^{1/2}$ and $\phi = \tan^{-1}(z/(r - r_0))$. Since we are primarily concerned with small displacements of the beam center, we consider only the $l = 1$ term in Eq. (20). Thus, the induced fields in Eq. (20) reduce to

$$\begin{aligned} B_r(t) &= -\frac{2I_0}{a^2 c} \int_0^t G_1(t-\tau) \Delta z(\tau) d\tau, \\ B_z(t) &= +\frac{2I_0}{a^2 c} \int_0^t G_1(t-\tau) \Delta r(\tau) d\tau, \end{aligned} \quad (21)$$

where the transform of $G_1(t)$ is given by Eq. (18).

IV. BEAM DYNAMICS

The externally applied fields associated with the modified betatron accelerator expanded about the center of the toroidal chamber $(r_0, 0)$, are

$$B_z = B_{0z}(1 - n(r - r_0)/r_0), \quad (22a)$$

$$B_r = -B_{0z}nz/r_0, \quad (22b)$$

and

$$B_\theta = B_{0\theta}(1 - (r - r_0)/r_0), \quad (22b,c)$$

where $B_{0z}, B_{0\theta}$ are constant and n is the external field index associated with the vertical field. Besides the external fields in Eq. (22), there are the induced electric and magnetic forces acting on the center of the beam, which is located at $r = r_0 + \Delta r(t)$ and $z = \Delta z(t)$. The induced magnetic field is given by Eq. (21). The induced electric field is not affected by a large but finite wall conductivity. Assuming an infinite wall conductivity, the induced electric field at the beam center is given by

$$\mathbf{E}(t) = \frac{2I_0}{v_0 a} \left(\frac{\Delta r(t)}{a} \hat{e}_r + \frac{\Delta z(t)}{a} \hat{e}_z \right). \quad (23)$$

Using the fields in Eqs. (21), (22) and (23), it can be shown that the transverse evolution of the beam center is governed by the equations

$$\begin{aligned} \Delta \ddot{r} + \frac{\Omega_{0z}^2}{\gamma_0^2} \xi_z (\Delta r - \Delta r_e) - \frac{\Omega_{0\theta}}{\gamma_0} \Delta \dot{z} &= \frac{-|e|\beta_0}{\gamma_0 m_0} B_z, \\ \Delta \ddot{z} + \frac{\Omega_{0z}^2}{\gamma_0^2} \xi_r \Delta z + \frac{\Omega_{0\theta}}{\gamma_0} \Delta \dot{r} &= \frac{|e|\beta_0}{\gamma_0 m_0} B_r, \end{aligned} \quad (24)$$

where a dot denotes the operation d/dt , $\beta_0 = v_0/c$, v_0 is the azimuthal velocity of the unperturbed beam centered at $r = r_0$ and $z = 0$, $\gamma_0 = (1 - \beta_0^2)^{-1/2}$, $\Omega_{0z} = |e|B_{0z}/m_0c$, $\Omega_{0\theta} = |e|B_{0\theta}/m_0c$, $\xi_z = 1 - n - 2(v/\gamma_0)(r_0/a)^2/\beta_0^2$ and $\xi_r = n - 2(v/\gamma_0)(r_0/a)^2/\beta_0^2$. The constant v is the Budker parameter and is given by

$$v = |e|^2 N / (2\pi m_0 c^2 r_0) = (\omega_b r_b / 2c)^2,$$

where $\omega_b^2 = 4\pi|e|^2 n_0 / m_0$. In Eq. (24), the term Δr_e is the equilibrium radial displacement of the beam's center and is given by

$$\Delta r_e = r_0 \frac{\delta\gamma/\gamma_0}{\xi_z},$$

where $\delta\gamma = \gamma - \gamma_0$ is proportional to the mismatch in beam energy. For $\delta\gamma = 0$, the beam center rotates about the center of the mirror cross section of the torus. Since we are concerned here with the relatively slow drift motion of the beam, i.e., $|\Delta \dot{r}| \ll |\Delta r|\Omega_{0z}/\gamma_0$ and $|\Delta \dot{z}| \ll |\Delta z|\Omega_{0z}/\gamma_0$, we may neglect the term $\Delta \dot{r}$ and $\Delta \dot{z}$ in Eq. (24).

Taking the Laplace transform of Eq. (24) in the drift approximation, i.e., $\Delta\ddot{r} = \Delta\ddot{z} = 0$, and rearranging terms, we find that

$$s\Delta\tilde{r}(s) - \Delta r(t=0) = -\frac{B_{0z}}{B_{0\theta}} \frac{\Omega_{0z}}{\gamma_0} [\xi_r \Delta\tilde{z}(s) - r_0 \tilde{B}_r(s)/B_{0z}], \quad (25a)$$

$$s\Delta\tilde{z}(s) - \Delta z(t=0) = \frac{B_{0z}}{B_{0\theta}} \frac{\Omega_{0z}}{\gamma_0} [\xi_z (\Delta\tilde{r}(s) - \Delta r_e/s) + r_0 \tilde{B}_z(s)/B_{0z}], \quad (25b)$$

where

$$\begin{aligned} r_0 \tilde{B}_r(s)/B_{0z} &= -2 \frac{v}{\gamma_0} \frac{r_0^2}{a^2} \tilde{G}_1(s) \Delta\tilde{z}(s), \\ r_0 \tilde{B}_z(s)/B_{0z} &= 2 \frac{v}{\gamma_0} \frac{r_0^2}{a^2} \tilde{G}_1(s) \Delta\tilde{r}(s). \end{aligned} \quad (26)$$

Substituting Eq. (26) into Eq. (25) gives

$$\begin{aligned} s\Delta\tilde{r}(s) - \Delta r(t=0) &= -\left[\omega_{Br} + \frac{2B_{0z}}{B_{0\theta}} \frac{\Omega_{0z}}{\gamma_0} \frac{v}{\gamma_0} \left(\frac{r_0}{a}\right)^2 (\tilde{G}_1(s) - 1) \right] \Delta\tilde{z}(s), \\ s\Delta\tilde{z}(s) - \Delta z(t=0) &= \left[\omega_{Bz} + 2 \frac{B_{0z}}{B_{0\theta}} \frac{\Omega_{0z}}{\gamma_0} \frac{v}{\gamma_0} \left(\frac{r_0}{a}\right)^2 (\tilde{G}_1(s) - 1) \right] \Delta\tilde{r}(s) \\ &\quad - \frac{B_{0z}}{B_{0\theta}} \frac{\Omega_{0z}}{\gamma_0} \xi_z \frac{\Delta r_e}{s}, \end{aligned} \quad (27)$$

where

$$\omega_{Br} = \frac{B_{0z}}{B_{0\theta}} \frac{\Omega_{0z}}{\gamma_0} \left(n - 2 \frac{v}{\gamma_0} \left(\frac{r_0}{a}\right)^2 (\beta_0 \gamma_0)^{-2} \right),$$

and

$$\omega_{Bz} = \frac{B_{0z}}{B_{0\theta}} \frac{\Omega_{0z}}{\gamma_0} \left(1 - n - 2 \frac{v}{\gamma_0} \left(\frac{r_0}{a}\right)^2 (\beta_0 \gamma_0)^{-2} \right).$$

Solving Eq. (27) for $\Delta\tilde{r}(s)$ and $\Delta\tilde{z}(s)$ with $n = 1/2$ and $\delta\gamma = 0$, we obtain

$$\begin{aligned} \Delta\tilde{r}(s) &= [s\Delta r(t=0) - \omega_B(1 + \tilde{\epsilon}(s))\Delta z(t=0)]/\tilde{D}(s), \\ \Delta\tilde{z}(s) &= [s\Delta z(t=0) + \omega_B(1 + \tilde{\epsilon}(s))\Delta r(t=0)]/\tilde{D}(s), \end{aligned} \quad (28)$$

where

$$\tilde{D}(s) = s^2 + \omega_B^2(1 + \tilde{\epsilon}(s))^2,$$

$$\tilde{\epsilon}(s) = s \frac{v}{\gamma_0} \frac{B_{0z}}{B_{0\theta}} \frac{\Omega_{0z}}{\gamma_0} \left(\frac{r_0}{a}\right)^2 (\tilde{G}_1(s) - 1)/\omega_B,$$

and

$$\omega_B = \omega_{Br} = \omega_{Bz} = \frac{B_{0z}}{B_{0\theta}} \frac{\Omega_{0z}}{\gamma_0} \left(\frac{1}{2} - 2 \frac{v}{\gamma_0} \left(\frac{r_0}{a} \right)^2 (\beta_0 \gamma_0)^{-2} \right).$$

V. DRAG INSTABILITY

The temporal evolution of the beam center is governed by the nature of the zeros of the function $\tilde{D}(s)$. We first note that for a perfect conducting chamber wall, $\sigma = \infty$, the function $\tilde{\epsilon}(s)$ vanishes since $\mu_1(s) \rightarrow \infty$ and hence $\tilde{G}_1(s) \rightarrow 1$. In this case the zeros of $\tilde{D}(s)$ are $s = \pm i\omega_B$, i.e., $\Delta r(t)$ and $\Delta z(t)$ are oscillatory with frequency ω_B . To analyze the dynamics of the beam for finite conducting walls we assume that the frequency shift and the growth rate are small in comparison with the bounce frequency ω_B , i.e., $s \approx \pm i\omega_B$. This comparison implies that $\tilde{\epsilon}(s) \ll 1$. Expanding $\tilde{D}(s) = 0$ about $s = s_0 = \pm i\omega_B$ gives

$$s = s_0 - \tilde{D}(s_0) \left/ \frac{\partial \tilde{D}(s)}{\partial s} \right|_{s=s_0}. \quad (29)$$

Substituting the expression for $\tilde{D}(s)$ into the right-hand side of Eq. (29) gives

$$s = s_0 - \omega_B^2 \tilde{\epsilon}(s_0) / s_0, \quad (30)$$

where

$$\tilde{\epsilon}(s_0) = 2 \frac{v}{\gamma_0} \frac{B_{0z}}{B_{0\theta}} \frac{\Omega_{0z}}{\gamma_0} \left(\frac{r_0}{a} \right)^2 (\tilde{G}_1(s_0) - 1) \omega_B^{-1},$$

and [from Eq. (18)],

$$\tilde{G}_1(s_0) - 1 = \frac{-2(\tanh \mu_1(s_0) + b\mu_1(s_0)/(b-a))}{2b\mu_1(s_0)/(b-a) + [1 + (b\mu_1(s_0)/(b-a))^2] \tanh \mu_1(s_0)}.$$

We now define the skin depth δ associated with a beam gyrating in the transverse plane with frequency ω_B as

$$\delta = \frac{c}{\sqrt{2\pi\sigma|\omega_B|}}.$$

In terms of δ , the function $\mu_1(s_0)$ is

$$\mu_1(s_0) = \sqrt{2} \left(\frac{b-a}{\delta} \right) \left(\frac{s_0}{|\omega_B|} \right)^{1/2}.$$

The zeros of $\tilde{D}(s)$ are approximately

$$s = \pm i\omega_B \pm i\lambda(\tilde{G}_1(\pm i\omega_B) - 1), \quad (31)$$

where

$$\lambda = 2 \frac{v}{\gamma_0} \frac{B_{0z}}{B_{0\theta}} \frac{\Omega_{0z}}{\gamma_0} \left(\frac{r_0}{a} \right)^2,$$

and

$$\mu_1(\pm i\omega_B) = \frac{b-a}{\delta} (1 \pm i\omega_B/|\omega_B|).$$

The dispersion relation, given by Eq. (31) is readily evaluated in the limit where $\delta < b-a$ and $\delta > b-a$.

Case (i) *Skin depth less than wall thickness* ($\delta < b-a$)

In this limit, Eq. (31) becomes

$$s = \pm i \left(\omega_B - \lambda \frac{\delta}{b} \right) - \lambda \frac{\delta}{b} \frac{\omega_B}{|\omega_B|}, \quad (32)$$

and the growth rate is

$$\Gamma = -\lambda \frac{\delta}{b} \frac{\omega_B}{|\omega_B|}, \quad (33)$$

i.e., is inversely proportional to the conductivity.

Case (ii) *Skin depth greater than wall thickness* ($\delta > b-a$)

For this limit, Eq. (31) becomes

$$s = \pm i\omega_B \mp i\lambda \frac{\left(1 \mp i \frac{\omega_B}{|\omega_B|} (b-a)b/\delta^2 \right)}{1 + ((b-a)b/\delta^2)^2}, \quad (34)$$

and the growth rate is

$$\Gamma = -\lambda \frac{\omega_B}{|\omega_B|} \frac{(b-a)b/\delta^2}{1 + (b-a)^2 b^2/\delta^4}.$$

For $[(b-a)b]^{1/2} > \delta > b-a$, the growth rate is

$$\Gamma = -\lambda \frac{\omega_B}{|\omega_B|} \frac{\delta^2}{(b-a)b}, \quad (35)$$

and is inversely proportional to the conductivity, while for $\delta > [(b-a)b]^{1/2}$ it is

$$\Gamma = -\lambda \frac{\omega_B}{|\omega_B|} \frac{(b-a)b}{\delta^2}, \quad (36)$$

and is proportional to the conductivity. In order for the beam to be unstable, the bounce frequency must be negative, i.e., $\omega_B < 0$. From the definition of ω_B , we find that the drag instability is stable if $v/\gamma_0 < (a/r_0)^2 \beta_0^2 \gamma_0^2 / 4$, which limits the beam current to

$$I_0 \leq I_{\text{crit}} \equiv 4.25(a/r_0)^2 \beta_0^2 \gamma_0^3 [\text{kA}]. \quad (37)$$

The general form of the growth rate as a function of the skin depth is depicted in Fig. 3.

The various expressions for the growth rate associated with the drag instability given by Eqs. (33), (35) and (36) can be conveniently expressed in terms of the parameter $x = I_0/I_{\text{crit}}$, where I_0 is the beam current and I_{crit} is given in Eq. (37). For $\delta/(b-a) < 1$, the normalized growth rate is

$$r_0 \Gamma / c = \lambda_0 \alpha_0 \left(\frac{b-a}{b} \right) \frac{x}{\sqrt{x-1}},$$

for $[b/(b-a)]^{1/2} > \delta/(b-a) > 1$,

$$r_0 \Gamma / c = \lambda_0 \alpha_0^2 \left(\frac{b-a}{b} \right) \frac{x}{x-1},$$

and for $\delta/(b-a) > [b/(b-a)]^{1/2}$,

$$r_0 \Gamma / c = \frac{\lambda_0}{\alpha_0^2} \left(\frac{b}{b-a} \right) x(x-1),$$

where $\delta/(b-a) \equiv \alpha_0/(|x-1|)^{1/2}$, $\lambda_0 = 0.12(B_{0z}/B_{0\theta})(r_0/a)^2 \gamma_0^{-1} I_{\text{crit}} [\text{kA}]$, $\alpha_0 = (\pi \sigma(B_{0z}/B_{0\theta})c/r_0)^{-1/2} c/(b-a)$ and $x \geq 1$.

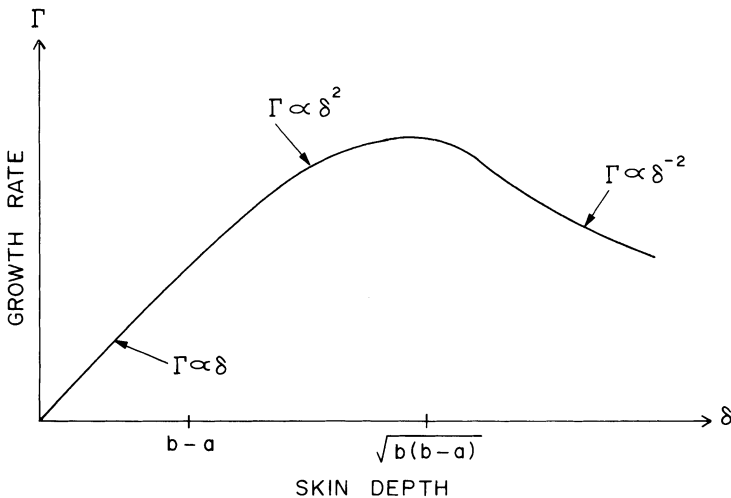


FIGURE 3 General form for the growth rate of the drag instability as a function of the skin depth in the modified betatron.

The NRL modified betatron is designed to operate at a beam current less than the critical current given in Eq. (37). This is necessary to avoid the drag instability, which could be severely destructive, as becomes apparent from the following numerical example. For $x = 2$, $a/r_0 = 1/10$, $r_0 = 100$ cm, $\gamma_0 = 6$, $(b - a) = 0.05$ cm, $B_{0z}/B_{0\theta} = 1/10$ and $\sigma = 2.5 \times 10^{15}$ sec $^{-1}$, the growth rate is approximately 8×10^6 sec $^{-1}$, i.e., the beam will strike the wall in less than a bounce period.

VI. SUMMARY AND CONCLUSIONS

The drag instability in the modified betatron is distinct from the beam-orbit instability, which may arise even for an infinite chamber-wall conductivity. The origin of the beam-orbit instability^{8,10} is due to an imbalance in the various confining forces, resulting in a net transverse drift velocity of the beam center and occurs even in the absence of dissipative forces. On the other hand, the drag instability arises from dissipative effects, i.e., finite conductivity. The instability condition associated with the beam orbit instability can be obtained from Eq. (27) by noting that for $\sigma = \infty$, unstable solutions occur for $\omega_{Br}\omega_{Bz} < 0$. However, if $n = 1/2$, $\omega_{Br}\omega_{Bz}$ is always equal to or greater than zero and the mode is stable. On the other hand, if $\sigma \neq \infty$ and $n = 1/2$ the drag instability is stable only if $\omega_B < 0$, i.e., $v/\gamma_0 < (a/r_0)^2\beta_0^2\gamma_0^2/4$. In a straight chamber, i.e., $r_0 = \infty$, this mode is always unstable.

In this paper, we have investigated the drag instability in a modified betatron geometry over a wide range of the parameter $\delta/(b - a)$. The maximum growth rate of the instability in high current accelerators could be much greater than the bounce frequency and thus the beam could strike the wall of the vacuum chamber in a time comparable to the bounce period. However, the drag instability is suppressed when the bounce frequency is positive, i.e., when $\omega_B > 0$. Therefore, it is necessary that during injection,²¹ the parameters of the experiment should be chosen in such a way that $\omega_B > 0$. It is important to point out that neither acceleration nor the diffusion of the self magnetic field can change the polarity of ω_B . For $\omega_B > 0$, the beam moves inward, i.e., toward the center of the minor cross section of this torus. This property might be used to drive the beam near the minor axis of the torus in a relatively short period of time after injection.²¹

ACKNOWLEDGMENT

The authors appreciate useful discussions with members of the Special Focus Program "Advanced Accelerator".

REFERENCES

1. T. J. Fessenden, et al, Proc. of the Intern. Top. Conf. on High-Power Electron and Ion Beam Research and Technology, Palaiseau, France, June 29–July 3, 1981, p. 813.
2. R. J. Briggs, et al., *IEEE Trans. Nucl. Sci.*, **NS-28**, 3360 (1981).
3. A.I. Paulovskii, et al, *Sov. Phys. Tech. Phys.*, **22**, 218 (1977).
4. A. G. Bonch-Osmolovskii, G. V. Dolbilov, I. N. Ivanov, E. A. Perelshtein, V. P. Sarantsev and O. I. Yarkovoy, JINR-Report P9-4135 Dubna (USSR) 1968.
5. P. Sprangle and C. A. Kapetanacos, *J. Appl. Phys.*, **49**, 1 (1978).
6. N. Rostoker, *Comments on Plasma Physics*, Gordon and Breach Science Publ. Inc. Vol. 6, p. 91 (1980).
7. C. L. Olson and V. Schumacher, *Collective Ion Acceleration* (Springer-Verlag, Berlin, Heidelberg, New York 1979), p. 199.

8. P. Sprangle, C. A. Kapetanakos and S. J. Marsh, Proc. of the Intern. Top Conf. on High-Power Electron and Ion Beam Research and Technology, Palaiseau, France, June 29–July 3, 1981, p. 803; also NRL Memo Report 4666 (1981).
9. G. Barak, D. Chernin, A. Fisher, H. Ishizuda, and N. Rostoker, Proc. of the Intern. Top Conf. on High Power Electron and Ion Beam Research and Technology, Palaiseau, France, June 29–July 3, 1981, p. 795.
10. C. A. Kapetanakos, P. Sprangle, D. P. Chernin, S. J. Marsh and I. Haber, *NRL Memo Report 4905* (1982); also *Phys. of Fluids* (1983).
11. H. S. Uhm and R. C. Davidson, MIT, Plasma Fusion Center Report No. JA-81-30 (1981).
12. H. H. Fleischmann, D. Taggart, M. Parker and H. J. Hopman, *Particle Accel. Conf. Bull.* page 146 Sante Fe, NM, 21–23 March (1983), (this ref. describes a plasma betatron, in which the electron ring is neutralized).
13. G. Barak and N. Roskoker, *Phys. of Fluids*, **26**, 3 (1983).
14. D. W. Kerst et al., *Rev. Sci. Instrum.*, **21**, 462 (1950).
15. D. W. Kerst, *Nature*, **157**, 90 (1940).
16. D. P. Chernin and P. Sprangle, *Particle Accelerators*, **12**, 85 (1982).
17. P. Sprangle and J. Vomvoridis, *NRL Memo Report 4688* (1981).
18. T. P. Hughes and B. B. Godfrey, Mission Research Corp. Report No. AMRC-R 354, 1982; also AMRC-R-332, 1982.
19. L. J. Laslett, V. K. Neil and A. M. Sessler, *Rev. Sci. Instrum.*, **36**, 436 (1965).
20. G. J. Caporeso, W. A. Berletta and V. K. Neil, *Particle Accelerators*, **11**, 71 (1980).
21. C. A. Kapetanakos, P. Sprangle and S. J. Marsh, *NRL Memo Report 4835* (1982); also *Phys. Rev. Lett.*, **49**, 741 (1982).